Surface-Enhanced Raman Spectroscopy in Single Living Cells Using Gold Nanoparticles

KATRIN KNEIPP,* ABIGAIL S. HAKA, HARALD KNEIPP, KAMRAN BADIZADEGAN, NORIKO YOSHIZAWA, CHARLES BOONE, KAREN E. SHAFER-PELTIER, JASON T. MOTZ, RAMACHANDRA R. DASARI, and MICHAEL S. FELD

Department of Physics, Technical University Berlin, D 10623 Berlin, Germany (K.K., H.K.); G. R. Harrison Spectroscopy Laboratory, Massachusetts Institute of Technology, Cambridge, Massachusetts 02139 (K.K., A.S.H., C.B., K.E.S.-P., J.T.M., R.R.D., M.S.F.); Department of Electrical Engineering and Computer Science, Massachusetts Institute of Technology, Cambridge, Massachusetts 02139 (K.K., N.Y.); and Department of Pathology, Children's Hospital and Harvard Medical School, Boston, Massachusetts 02115 (K.B.)

Ultrasensitive Raman measurements in single living cells are possible through exploiting the effect of surface-enhanced Raman scattering (SERS). Colloidal gold particles (60 nm in size) that are deposited inside cells as "SERS-active nanostructures" result in strongly enhanced Raman signals of the native chemical constituents of the cells. Particularly strong field enhancement can be observed when gold colloidal particles form colloidal clusters. The strongly enhanced Raman signals allow Raman measurements of a single cell in the 400–1800 cm^{-1} range with 1-μm lateral resolution in relatively short collection times (1 second for one mapping point) using 3–5 mW near-infrared excitation. SERS mapping over a cell monolayer with 1-μm lateral resolution shows different Raman spectra at almost all places, reflecting the very inhomogeneous chemical constitution of the cells. Colloidal gold supported Raman spectroscopy in living cells provides a tool for sensitive and structurally selective detection of native chemicals inside a cell, such as DNA and phenylalanine, and for monitoring their intracellular distributions. This might open up exciting opportunities for cell biology and biomedical studies.

Index Headings: **Surface-enhanced Raman scattering; Gold colloids; Cells; DNA.**

INTRODUCTION

Raman scattering is a vibrational spectroscopic technique in which incident laser light is inelastically scattered from a sample and shifted in frequency by the energy of its characteristic molecular vibrations. The Raman spectrum provides high informational content on the chemical structure of the probed substances, which makes this method a very promising tool in biomedical spectroscopy.[1,2]

Within the recent decade, Raman spectroscopy was also successfully applied to living cells.[3–9] Measurements on cell monolayers using confocal Raman systems with about 1-μm spatial resolution show clear differences in the Raman spectra of the cell nucleus and the cell cytoplasm.[3–9] Excellent Raman spectra of DNA in the nucleus of a living cell are measured using a laser Raman microscope, where the sample is inside the laser cavity.[4]

Raman scattering is an inefficient effect, with typical nonresonant Raman cross-sections on the order of 10^{-30} cm^2 per molecule. Since many chemicals are present in a cell at very low concentrations and since the applicable excitation laser intensity is limited by effects of cell degeneration, the Raman signal observed from a single cell is extremely weak. Typical collection times for a spontaneous Raman spectrum inside a living cell using 5–10 mW laser excitation in a confocal Raman system can be hundreds of seconds, summing up to very long data acquisition times for a "Raman map" of a cell, thus making it difficult to study viable cell lines.[9]

In surface-enhanced Raman scattering (SERS), Raman signals can be enhanced by many orders of magnitude when the probed molecules are attached to metallic nanostructures and Raman scattering takes place in the high local optical fields of these structures.[1,10–13] Areas of enhanced local optical fields occur due to resonances of the applied optical fields with the surface plasmon oscillations of the metallic nanostructures. In addition to this "electromagnetic field enhancement," the electronic interaction between the Raman molecule and the metal can result in an increase of the Raman cross-section itself, called "chemical or electronic enhancement." Several mechanisms are discussed to account for this chemical SERS enhancement, such as a resonance Raman effect, which becomes operative due to possibly shifted and broadened electronic levels in the adsorbed molecule compared to the "free" one or due to a new (charge transfer) electronic transition in the metal–molecule system.[10,13] In many experiments on nanometer-scaled silver or gold structures, the "chemical effect" provides a very small contribution and the total SERS enhancement is determined by electromagnetic field enhancement.[1,14–17] In the visible and near-infrared frequency range, silver and gold colloidal clusters or island films of these materials can result in electromagnetic SERS enhancement factors up to 10 or 12 orders of magnitude.[14–17]

Of course, the field enhancement effect is also operative in fluorescence. The effect of surface-enhanced fluorescence has been observed for a few molecules/ions.[18–21] However, in many cases, the metal provides strong nonradiative decay channels. This fluorescence quenching effect can overcompensate the field enhancement, and the net fluorescence signal observed for molecules attached to a metallic nanostructure is much smaller than that measured without the metal. That also explains why in many experiments the surface-enhanced resonance Raman

Received 26 September 2001; accepted 12 November 2001.

* Author to whom correspondence should be sent. E-mail kneipp@usa.net.

0003-7028/02/5602-0150$2.00/0

(SERRS) spectrum does not show the expected fluorescence background.[22–25]

SERS studies have also been performed on living cells.[26–29] In these experiments, colloidal silver particles were incorporated inside the cells and SERS was applied to monitor the intracellular distribution of drugs in the whole cell and to study the antitumor drugs/nucleic acid complexes. Surprisingly, these experiments show SERS spectra of the drugs/DNA complex represented by Raman lines of the drugs, but no SERS spectra of the native cell constituents themselves were detected. Weak SERS bands attributed to phenylalanine and amide I and III bands were measured in the strong SERS spectra of dimethylcrocetin (DMCRT) in a living HL 60 cell in contact with a gold island film.[30] In Ref. 31, silver nanocolloids were produced selectively within *Escheri coli* bacteria or on its wall, resulting in SERS spectra of the constituents forming the cell wall, such as proteins, peptides, and amino acids.

In general, due to its chemical inactivity, gold should be the more suitable metal for incorporation inside living cells. It was shown that gold colloidal clusters have comparably good SERS enhancement factors as silver clusters when near-infrared (NIR) excitation is applied.[32] Moreover, NIR would be the desired excitation range for Raman measurements of cells because the lower-energy photons reduce the fluorescence background in biological samples and also the risk of cell degeneration.[2,9]

In this paper we report NIR-SERS studies inside living cells using colloidal gold as the SERS active substrate. In contrast to previous SERS studies inside living cells using colloidal silver, we measure strong SERS signals from the native chemical constituents of a cell. In this way, this work should provide a tool for the sensitive and structurally selective detection of native chemicals inside a cell and their intracellular distribution, suggesting many applications in biomedical research.

EXPERIMENTAL

Differentiated intestinal epithelial cells HT29 (gift of the Harvard Digestive Diseases Center) were grown either on 25-mm round coverglasses or on formvar-carbon coated electron microscopy grids using high-glucose Dulbecco's modified Eagle medium (DMEM) supplemented with 10% fetal calf serum, 100 units/mL penicillin, and 100 μg/mL streptomycin (all Gibco BRL products, Life Technologies, Grand Island, NY). Cells were grown to confluency at 37 °C in a humidified atmosphere of 5% CO_2 in air. Monolayers were loaded with colloidal gold either by sonication (see below) or by fluid-phase uptake. For fluid-phase uptake, approximately 24 hours before the experiments the culture medium was supplemented with the colloidal gold suspension either at approximately 3300 particles per cell or at 330 particles per cell. Immediately before the experiments, free gold was removed by rinsing the monolayers in Hank's Balanced Salt Solution (HBSS) without sodium bicarbonate or phenol red, buffered at pH 7.4 with 10 mM HEPES (both from Sigma, St. Louis, MO). Cells remained in the same buffer throughout the measurements. Another method for incorporating gold nanoparticles into the cell is by sonication.

Ultrasound has been shown to rupture the cell plasma membrane and permit entry of the colloidal gold particles, followed be self-annealing of the ruptured membrane edges within a few seconds. Raman spectra shown in this work are taken from cells in which 60-nm gold nanoparticles were incorporated in the cells by fluid-phase uptake during the growing process. The salts in the buffer solution induce the formation of small colloidal aggregates with sizes of a few hundred nanometers. Cluster–cluster aggregation inside the cell results in the formation of larger gold colloidal clusters, as we discuss below. Evidence that cells are alive after treatment with the colloidal gold comes from phase contrast inspection of the cultures showing that cells incubated with colloidal gold are visibly growing and that there is no evidence of cell rounding, apoptotic activity, or cell detachment from the growth surface when compared with control monolayers.

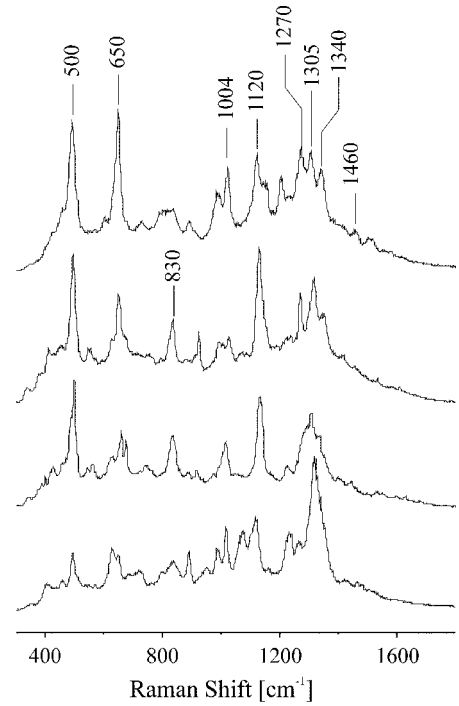

FIG. 1. Typical unprocessed surface-enhanced Raman spectra measured with 1-μm spot size at different places on a cell monolayer incubated with colloidal gold.

Raman measurements were carried out on single cells using a microscope for focusing the 830-nm excitation laser to a spot size of about 1 μm. The same microscope objective was also used for collecting the Raman scattered light. A single stage spectrograph and a charge-coupled device (CCD) detector were used for spectral dispersion and collection of the scattered light. Application of 2–5 mW of near-infrared excitation did not result in any cell degeneration. Good signal-to-noise SERS spectra were measured in one second collection time. For mapping experiments, the cell monolayer sample was moved in 1-μm raster steps under the laser focus covering an area of 30 × 30 μm^2. The experimental system is described in more detail in Ref. 9.

RESULTS AND DISCUSSION

Figure 1 shows typical unprocessed surface-enhanced Raman spectra measured with 1-μm spot size within the

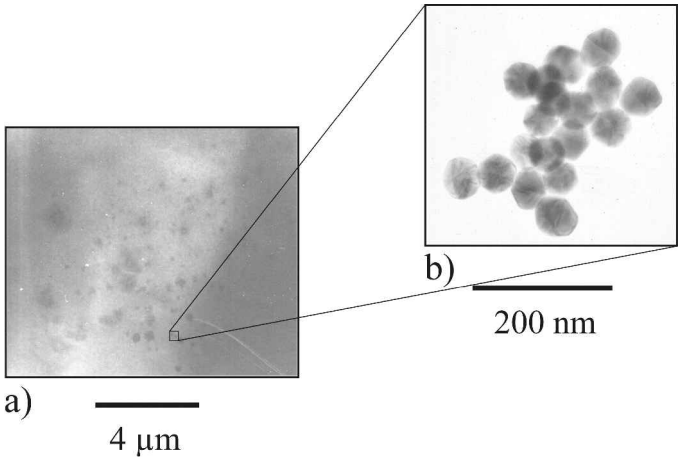

FIG. 2. Electron micrographs of colloidal gold particles inside a cell monolayer (**a**). The higher magnification shows that the gold particles are aggregates of 60-nm colloidal spheres (**b**).

$30 \times 30\ \mu m^2$ area at different places on a cell monolayer incubated with colloidal gold. The one second collection time spectra show a very good signal-to-noise ratio, allowing for the possibility of much shorter collection times. The SERS signal appears on the order of thousands of counts per second compared to signals of counts per second measured in ''normal'' Raman spectroscopy of single cells.

The Raman lines can be assigned to native chemical constituents in the cell nucleus and cytoplasm, such as DNA, RNA, phenylalanine, tyrosine, etc. In general, all 900 spectra measured at different places are distinct, reflecting the inhomogenity of a cell. As Fig. 1 shows, differences between the spectra appear regarding relative Raman amplitudes and Raman line width and sometimes also regarding several weaker Raman lines, which contribute to the spectra.

The 1120 cm^{-1} line can be assigned to an O–P–O DNA backbone vibration,[3,4] where this line is slightly shifted to larger wave numbers in SERS compared to ''normal'' Raman scattering.[33] Raman lines around 1300 cm^{-1} are related to adenine and guanine vibrations, but RNA also has strong surface-enhanced Raman bands in this frequency region.[34] The spectral region around 1000 cm^{-1} is determined by phenylalanine (1004 cm^{-1}) and a C–O DNA backbone vibration at 980 cm^{-1}. The bands at about 830 cm^{-1} can be assigned to a sugar–phosphate backbone vibration, where the frequency of this line is slightly different for B- and A-form DNA.[4] The absence of a strong SERS line at 735 cm^{-1}, which relates to the adenine ring breathing mode, indicates that native, and not denatured, DNA contributes to the spectra.[33,35]† SERS spectra also show the conformationally sensitive guanine lines around 650/670 cm^{-1}.[4] The strong SERS line at 650 cm^{-1} in the upper spectrum is very likely due to a superposition of a strong tyrosine vibration[4] and the guanine line.

SERS can be a selective effect showing predominately those molecules or molecular groups that are in the very close vicinity of the colloidal gold clusters.[31–35] In contrast to ''normal'' Raman spectra of living cells, where strong Raman bands appear around 1450 cm^{-1} (protein CH deformation vibration) and at 1650 cm^{-1} (amide I), in the SERS spectra of living cells these bands seem to exhibit almost no enhancement. In a few spectra, a very weak SERS band appears at about 1450 cm^{-1}.

Figure 2 shows electron micrographs of the colloidal gold particles inside a cell monolayer. The colloidal particles form small colloidal clusters in sizes between 100 nm and a few micrometers, where the largest clusters can also be seen in the phase contrast microscope views in Fig. 3. The higher magnification in Fig. 2b shows that the gold clusters are made of 60 nm colloidal gold spheres. From NIR-SERS experiments performed on calf thymus DNA attached to such gold colloidal cluster, we can infer a minimum enhancement factor of 10^3–10^4 for DNA on colloidal gold based on the assumption that all DNA molecules in the sample contribute to the SERS signal.[1] SERS spectra and enhancement factors of DNA

† In SERS spectra of DNA, for an open double strand, the 735 cm^{-1} band appears stronger due to better contact between the bases and the colloidal gold or silver compared to native DNA. The appearance of the strong adenine ring breathing line therefore indicates denaturation of the DNA.[33,35]

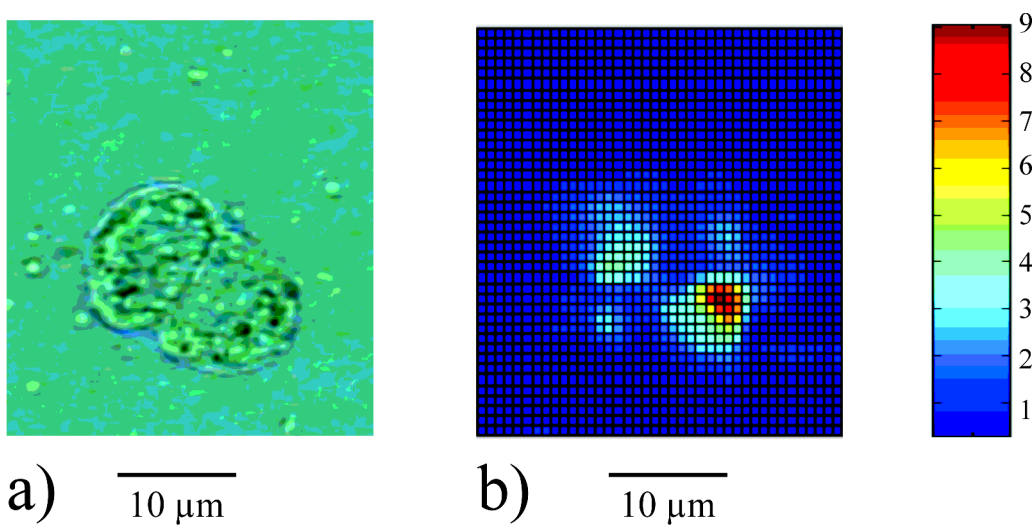

FIG. 3. Phase contrast image of two living cells (**a**) and the image of the total SERS signal (**b**).

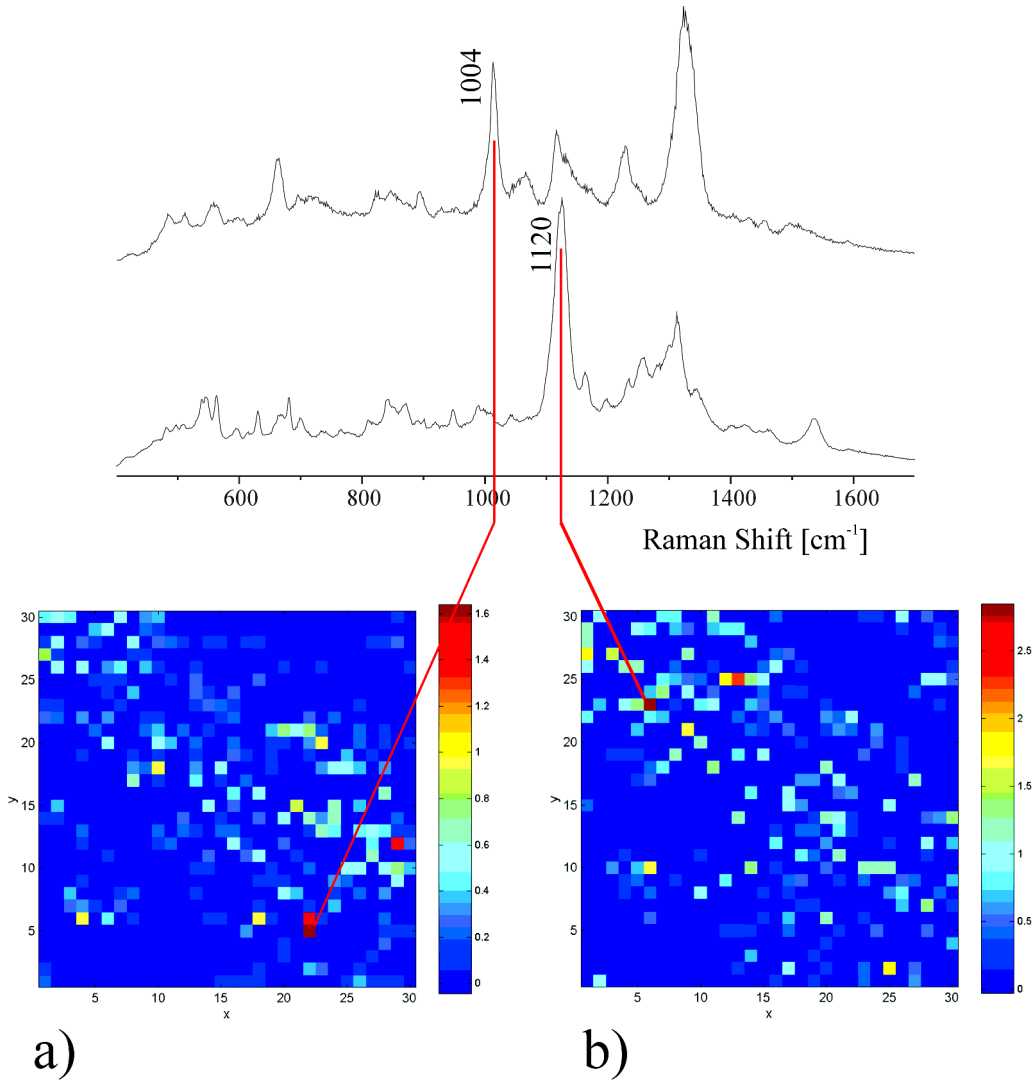

FIG. 4. Distribution of phenylalanine (**a**) and DNA (**b**) over a 30 × 30 μm² cell monolayer based on the signals of the 1004 cm^{-1} Phe– (**a**) and 1120 cm^{-1} O–P–O DNA backbone (**b**) line. SERS spectra are measured at the places of the maximum signals of the two peaks.

on colloidal gold clusters are in agreement with results on colloidal silver clusters.[33]

Figure 3 shows a comparison between a phase contrast image of two living cells on a glass plate and the image of the total Raman signal. The figure shows that the SERS signal does not appear over the entire cell and that parts of the cell show no Raman signal. Since it is unlikely that there are regions of the cell that do not contain Raman scatterers, it follows that the lack of a SERS signal results from the absence of colloidal gold particles in those regions. The variations in the scattering signal power in the ''SERS-active'' or gold occupied cell regions may appear due to a nonuniform electromagnetic SERS enhancement factor inside the cell or may also reflect a very inhomogeneous distribution of the scattering substance inside the cell. At this point, we cannot separate these two effects.

In order to solve this problem and to image a particular substance using SERS, the signal of a specific Raman line must be normalized to the SERS enhancement factor operative at the appropriate location. The surface-enhanced Raman lines appear on a broad background, which we ascribe to ''surface-enhanced'' fluorescence signal of the cell. With the applied 830-nm excitation, the cell fluorescence is certainly only weakly excited and it might additionally be quenched by the colloidal gold; but, on the other hand, fluorescence also takes place in enhanced local fields, as was briefly discussed in the introduction. Therefore, the lateral distribution of the broad fluorescence signal (with contributions from many fluorophores) should monitor the distribution of the field enhancement. Therefore, the signals are normalized to the average fluorescence signal between 400 and 1700 cm^{-1} relative to the 830-nm excitation.

As an example of SERS imaging, Figs. 4a and 4b show the distribution of phenylalanine and DNA over a 30 × 30 μm² cell monolayer based on the normalized signals of the 1004 cm^{-1} Phe– and 1120 cm^{-1} O–P–O DNA backbone line, respectively. Also shown in Fig. 4 are SERS spectra taken from regions of the maximum signals of the two lines. In general, the cell nucleus should contain a larger amount of DNA, whereas phenylalanine should be mainly present in the cytoplasm,[3,9] which explains why the maximum signals of the two Raman lines

appear at different places. It should be noted that the SERS image over a cell monolayer shown in Figs. 4a and 4b, of course, shows the distribution of the native cell constituents only in regions where colloidal gold is present. For further developing this spectroscopic technique, technologies should be explored that generate a uniform distribution of the SERS-active nanostructures over the cell.

To summarize, the reported experiments demonstrate the feasibility of measuring surface-enhanced Raman spectra of native constituents within a single viable cell using colloidal gold particles as SERS-active nanostructures and generating a surface-enhanced Raman image inside a living cell. The strong Raman signal allows Raman mapping over a single cell in very short times compared to normal Raman measurements and provides also the opportunity of Raman screening of many cells in relatively short times. A SERS spectrum provides rich structural information about the cell and allows observation of small structural modifications, such as changes in the DNA bands. In this way, ultrasensitive Raman spectroscopy inside living cells opens up interesting new opportunities for the diagnosis of diseases at a very early stage, as it should allow for monitoring small chemical changes in the cell that could be the precursors of larger morphological changes, visible by conventional microscopy. Based on the structural sensitivity and the capability of relatively fast screening of many cells, exciting opportunities are opened up for the diagnosis of diseases such as cancer to be made at earlier stages than previously possible.

ACKNOWLEDGMENTS

This work was supported by NIH and BMBF grants. We would like to thank the editor and the reviewers for valuable comments and suggestions.

1. K. Kneipp, H. Kneipp, I. Itzkan, R. R. Dasari, and M. S. Feld, Chem. Rev. **99,** 2957 (1999).
2. E. B. Hanlon, R. Manoharan, T. W. Koo, K. E. Shafer, J. T. Motz, M. Fitzmaurice, J. R. Kramer, I. Itzkan, R. R. Dasari, and M. S. Feld, Phys. Med. Biol. **45,** R1 (2000).
3. G. J. Puppels, F. F. M. de Mull, C. Otto, J. Greve, M. Robert-Nicoud, D. J. Arndt-Jovin, and T. M. Jovin, Nature (London) **372,** 301 (1990).
4. W. L. Peticolas, T. W. Patapoff, G. A. Thomas, J. Postlewait, and J. W. Powell, J. Raman Spectrosc. **27,** 571 (1996).
5. C. Otto, C. J. de Grauw, J. J. Duindam, N. M. Sijtsema, C. Otto, and J. Greve, J. Raman Spectrosc. **28,** 143 (1997).
6. N. M. Sijtsema, C. Otto, G. M. J. Segers-Nolten, A. J. Verhoeven, and J. Greve, Biophys. J. **74,** 3250 (1998).
7. A. V. Feofanov, A. I. Grichine, L. A. Shitova, T. A. Karmakova, R. A. Yakubovskaya, M. Egret-Charlier, and P. Vigny, Biophys. J. **78,** 499 (2000).
8. N. M. Sijtsema, A. G. J. Tibbbe, J. Segers-Nolten, A. J. Verhoeven, R. S. Weening, J. Greve, and C. Otto, Biophys. J. **78,** 2606 (2000).
9. K. E. Shafer-Peltier, A. S. Haka, M. Fitzmaurice, J. Crowe, J. Myles, R. R. Dasari, and M. S. Feld, J. Raman Spectrosc., paper submitted.
10. A. Otto, ''Surface-Enhanced Raman Scattering: 'Classical' and 'Chemical' Origins'', in *Light Scattering in Solids IV,* M. Cardona and G. Guntherodt, Eds. (Springer-Verlag, Berlin, Germany, 1984), vol. 1984, p. 289.
11. M. Moskovits, Rev. Mod. Phys. **57,** 783 (1985).
12. K. Kneipp, Experimentelle Technik der Physik **38,** 1 (1990).
13. A. Campion and P. Kambhampati, Chem. Soc. Rev. **27,** 241 (1998).
14. K. Kneipp, Y. Wang, H. Kneipp, L. T. Perelman, I. Itzkan, R. R. Dasari, and M. S. Feld, Phys. Rev. Lett. **78,** 1667 (1997).
15. K. Kneipp, H. Kneipp, I. Itzkan, R. R. Dasari, and M. S. Feld, Proc. SPIE-Int. Soc. Opt. Eng. **4258,** 50 (2001).
16. K. Kneipp, H. Kneipp, V. B. Kartha, R. Manoharan, G. Deinum, I. Itzkan, R. R. Dasari, and M. S. Feld, Phys. Rev. E: Stat. Phys., Plasmas, Fluids, Relat. Interdiscip. Top. **57,** R6281 (1998).
17. K. Kneipp, H. Kneipp, G. Deinum, I. Itzkan, R. R. Dasari, and M. S. Feld, Appl. Spectrosc. **52,** 175 (1998).
18. D. A. Weitz, S. Garoff, J. I. Gersten, and A. Nitzan, J. Chem. Phys. **78,** 5324 (1983).
19. K. Sokolov, G. Chumanov, and T. M. Cotton, Anal. Chem. **70,** 3898 (1998).
20. S. T. Selvan, T. Hayakawa, and M. Nogami, J. Phys. Chem. B **103,** 7064 (1999).
21. C. J. L. Constantino and R. F. Aroca, J. Raman Spectrosc. **31,** 887 (2000).
22. A. Bachackashvilli, S. Efrima, B. Katz, and Z. Priel, Chem. Phys. Lett. **94,** 571 (1983).
23. K. Kneipp, G. Hinzmann, and D. Fassler, Chem. Phys. Lett. **99,** 5 (1983).
24. B. Pettinger, Chem. Phys. Lett. **110,** 576 (1984).
25. A. Bacackashvilli, B. Katz, Z. Priel, and S. Efrima, J. Phys. Chem. **88,** 6185 (1984).
26. M. Manfait, H. Morjani, J. M. Millot, V. Debal, J. F. Angiboust, and I. Nabiev, Proc. SPIE-Int. Soc. Opt. Eng. **1403,** 695 (1990).
27. M. Manfait, H. Morjani, and I. Nabiev, J. Cell. Pharmaco. **3,** 120 (1992).
28. I. Nabiev, H. Morjani, and M. Manfait, Eur. Biophys. J. **19,** 311 (1991).
29. H. Morjani, J. F. Riou, I. Nabiev, F. Lavelle, and M. Manfait, Cancer Res. **53,** 4784 (1993).
30. A. Beljebbar, G. D. Sockalingum, H. Morjani, and M. Manfait, Proc. SPIE-Int. Soc. Opt. Eng. **3608,** 175 (1999).
31. S. Efrima and B. V. Bronk, J. Phys. Chem. **102,** 5947 (1998).
32. K. Kneipp, H. Kneipp, R. Manoharan, E. B. Hanlon, I. Itzkan, R. R. Dasari, and M. S. Feld, Appl. Spectrosc. **52,** 1493 (1998).
33. K. Kneipp and J. Flemming, J. Mol. Struct. **145,** 145 (1986).
34. K. Kneipp, W. Pohle, and H. Fabian, J. Mol. Struct. **244,** 183 (1991).
35. G. Chumanov and T. M. Cotton, Proc. SPIE-Int. Soc. Opt. Eng. **3608,** 204 (1999).